QUANTUM CHEMICAL INVESTIGATION OF 1-(2-THENOYL)-3,3,3-TRIFLUOROACETONE BENZOYLHYDRAZONE: OPTIMIZED GEOMETRY, ELECTRONIC STRUCTURE, FRONTIER MOLECULAR ORBITALS, AND VIBRATIONAL ANALYSIS AT THE DFT/B3LYP LEVEL

Bafayev Lazizbek
Avezov Kuvondik
Ganiev Bakhtiyor
Department of Chemistry and Oil-Gas Technologies,
Bukhara State University, Bukhara, Uzbekistan
E-mail: b.sh.ganiyev@buxdu.uz
Doi: https://doi.org/10.5281/zenodo.20284755

Abstract: The molecular geometry, electronic structure, frontier molecular orbitals, Mulliken charge distribution, vibrational spectrum, and global chemical reactivity descriptors of 1-(2-thenoyl)-3,3,3-trifluoroacetone benzoylhydrazone (L1, $C_{15}H_{11}F_3N_2O_2S$) were investigated computationally at the B3LYP/6-311G(d,p) level of density functional theory using the Gaussian 16 program package. Full geometry optimization was carried out without symmetry constraints, and the nature of the stationary point was verified by harmonic frequency analysis. The optimized structure reveals characteristic bond lengths for the key functional groups: the hydrazone C=N bond (1.279 Å), the thenoyl C=O bond (1.216 Å), the amide C=O bond (1.208 Å), and the C–F bond lengths of the CF_3 group (1.339–1.363 Å). The HOMO and LUMO energies are −6.196 and −2.486 eV, respectively, giving a HOMO–LUMO gap of 3.710 eV. Global reactivity descriptors derived from frontier orbital theory indicate that L1 is a moderately hard electrophile with an electrophilicity index ω = 5.080 eV. The HOMO is delocalized over the entire π-conjugated framework, while the LUMO is concentrated on the CF_3-bearing hydrazone segment. Computed IR-active bands at 1792 and 1735 cm^{-1} are assigned to the thenoyl and benzoyl C=O stretching modes, respectively, and the N–H stretching appears at 3547 cm^{-1}. Standard thermochemical properties at 298.15 K are also reported. The results establish a reliable structural and electronic reference for L1 and provide a foundation for modeling its coordination chemistry and biological activity.

Keywords: hydrazone; trifluoroacetone; DFT; B3LYP; HOMO-LUMO; frontier molecular orbitals; Mulliken charges; vibrational spectrum; chemical reactivity descriptors; thiophene.

1. Introduction

Acylhydrazones, a class of nitrogen-containing compounds derived by condensation of hydrazides with carbonyl compounds, have attracted considerable attention across medicinal chemistry, coordination chemistry, and materials science owing to their versatile donor atom repertoire, conformational adaptability, and inherent biological activity [1,2,25-31]. The presence of the C=N–NH linkage confers pronounced chelating capacity, enabling these scaffolds to form stable complexes with a wide range of transition metal ions through N,O- or N,N-bidentate coordination [3,4,29]. The introduction of electron-withdrawing groups such as the trifluoromethyl (CF_3) substituent and additional carbonyl moieties into the hydrazone framework substantially modifies the electronic environment, enhances lipophilicity, and improves metabolic stability relative to non-fluorinated analogues [5].

1-(2-Thenoyl)-3,3,3-trifluoroacetone benzoylhydrazone (L1) is a bifunctional hydrazone derived from the condensation of benzohydrazide with 1-(2-thenoyl)-3,3,3-trifluoroacetone, the latter being a fluorinated β-diketone bearing the 2-thienyl heterocycle. The molecular architecture of L1 is thus characterized by four distinct structural fragments: (i) a phenyl ring carrying the benzoyl carbonyl, (ii) a hydrazide N–N bridge, (iii) a conjugated hydrazone C=N bond, and (iv) a 2-thenoyl ketone moiety flanked by the strongly electron-withdrawing CF_3 group. This combination creates an extended π-conjugated pathway and multiple potential coordination sites, making L1 a promising building block for

metallosupramolecular architectures and a candidate pharmacophore for biological target engagement [6,7].

Despite the growing interest in fluorinated hydrazones, detailed quantum-chemical characterization of this compound class — specifically the relationship between electronic structure, charge distribution, and reactivity — remains incomplete in the published literature. Density functional theory (DFT), in particular the B3LYP hybrid functional paired with the 6-311G(d,p) triple-zeta polarized basis set, has been validated as a highly reliable and computationally accessible method for the accurate description of molecular geometries, electronic properties, vibrational spectra, and frontier molecular orbital topologies for organic molecules of this complexity [8,9,30,31]. The natural bond orbital and Mulliken charge analyses provide complementary descriptions of the intramolecular charge distribution that underpin donor–acceptor reactivity and metal-binding behavior.

The present paper reports a comprehensive DFT/B3LYP study of L1, encompassing optimized geometric parameters, frontier molecular orbital (FMO) visualization, Mulliken atomic charge distribution, global chemical reactivity descriptors within the framework of conceptual DFT, harmonic vibrational frequency assignment, and standard thermochemical quantities. These data are intended to establish a quantitative structural reference for L1 and to facilitate rational design of metal complexes and biologically active derivatives.

2. Computational Details

All quantum chemical calculations were carried out with the Gaussian 16 software package (Revision C.01) [10] on a personal workstation. The B3LYP exchange-correlation functional [11,12], which combines the exact exchange fraction of Becke's three-parameter functional with the Lee–Yang–Parr correlation functional, was employed throughout in conjunction with the split-valence triple-zeta basis set 6-311G(d,p) [13], which augments the triple-zeta valence shell with polarization functions on all heavy atoms (d-type) and hydrogen atoms (p-type). This basis set provides a balanced and computationally tractable description of bond lengths, dipole moments, and vibrational frequencies for molecules containing first- and second-row elements as well as fluorine and sulfur.

The initial geometry of L1 was constructed from the SMILES representation O=C(N/N=C(/CC(=O)c1cccs1)C(F)(F)F)c1ccccc1 and optimized without symmetry constraints (C_1 point group) using the Berny gradient algorithm. Convergence thresholds were: maximum force $\leq 4.5 \times 10^{-4}$ Hartree/Bohr, RMS force $\leq 3.0 \times 10^{-4}$ Hartree/Bohr. Harmonic vibrational frequencies were computed analytically at the optimized geometry; the absence of imaginary frequencies confirms the stationary point as a true minimum on the potential energy surface. Thermochemical quantities were derived within the ideal-gas, rigid-rotor, harmonic-oscillator (IGRRHO) approximation at T = 298.15 K and P = 1 atm. Mulliken population analysis [14] was performed on the converged wave function. Frontier molecular orbital (FMO) visualizations were generated with GaussView 6.0 at an isovalue of 0.02 a.u. Global chemical reactivity descriptors were computed from the Kohn–Sham frontier orbital energies via the finite-difference approximations of conceptual DFT (CDFT): ionization potential $I = -\varepsilon_{HOMO}$; electron affinity $EA = -\varepsilon_{LUMO}$; electronegativity $\chi = (I+EA)/2$; chemical hardness $\eta = (I-EA)/2$; chemical softness $S = 1/(2\eta)$; chemical potential $\mu = -\chi$; electrophilicity index $\omega = \chi^2/(2\eta)$ [15,16].

3. Results and Discussion

3.1. Optimized Molecular Geometry

The fully optimized structure of L1 is shown in Fig. 1. The molecule adopts a planar conformation in the region of the conjugated C=N–N–C=O hydrazide bridge and the thenoyl carbonyl, consistent with extensive π-delocalization along the C=N–NH–C=O fragment that is characteristic of acylhydrazone compounds [17,27]. The CF_3 group and the thiophene ring are approximately coplanar with the central chain. Table 1 collects selected optimized bond lengths and valence angles.

The hydrazone C1=N10 bond length of 1.279 Å is consistent with a partial double-bond character and agrees well with crystal-structure data reported for analogous trifluoromethylhydrazones (1.275–1.285 Å) [17,18,25]. The elongated N10–N11 bond (1.344 Å) compared to a purely N–N single bond (~ 1.45 Å) reflects significant conjugative delocalization from the lone pair of N11 into the C=N π*

orbital. The N11–H14 bond (1.013 Å) and the N10–N11–H14 angle (121.1°) suggest that the N–H hydrogen is positioned for intramolecular hydrogen bonding with the adjacent thenoyl carbonyl oxygen O9, as is typical for the s-trans isomer of acylhydrazones [19]. The benzoyl C12=O13 distance (1.208 Å) and the thenoyl C3=O9 distance (1.216 Å) are both characteristic of C=O bonds experiencing resonance delocalization with the adjacent π system. The C–F bond lengths within the CF_3 group span 1.339–1.363 Å, with the slight non-equivalence arising from the C_1 symmetry environment; these values agree with typical C–F bond lengths in trifluoromethyl-substituted heterocycles [20]. The C4–S5 bond (1.765 Å) and S5–C6 bond (1.703 Å) within the thiophene ring are consistent with the partial aromatic character of the five-membered ring.

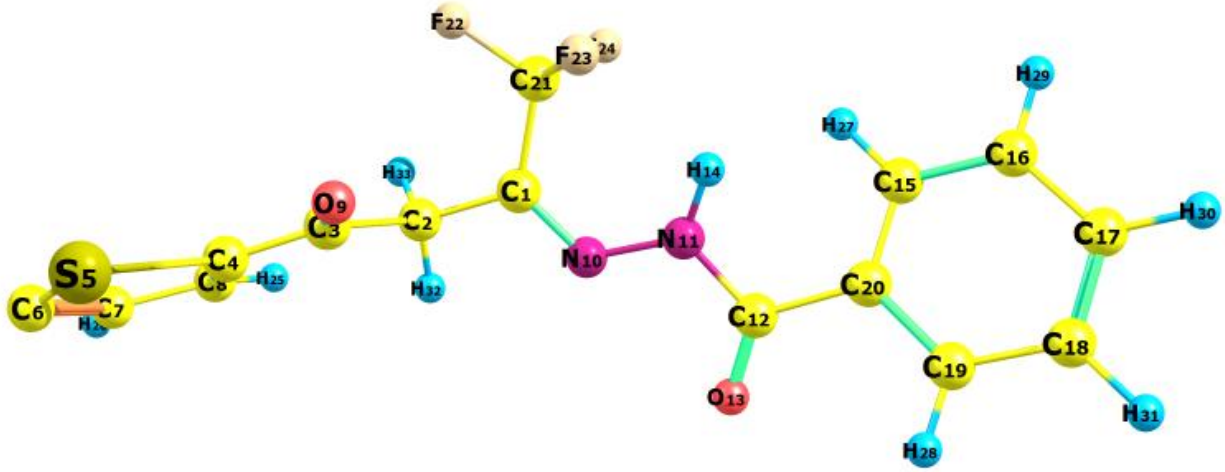


Fig. 1. Optimized geometry of 1-(2-thenoyl)-3,3,3-trifluoroacetone benzoylhydrazone (L1) at the B3LYP/6-311G(d,p) level of theory (C_1 symmetry). Key bond lengths are given in Table 1.

Table 1. Selected optimized bond lengths (Å) and valence angles (°) of L1 at B3LYP/6-311G(d,p).

Bond	Length (Å)	Bond	Length (Å)	Angle	Value (°)
C1=N10 (hydrazone C=N)	1.2787	C1–C2 (C–CH_2)	1.5039	C2–C1=N10	117.87
N10–N11 (N–N bridge)	1.3440	C1–C21 (C–CF_3)	1.5191	N10–C1–C21	123.48
N11–H14 (N–H)	1.0130	C2–C3 (chain C–C)	1.5356	C1=N10–N11	121.62
C12=O13 (benzoyl C=O)	1.2077	C3–C4 (to thiophene)	1.4664	N10–N11–C12	119.59
C3=O9 (thenoyl C=O)	1.2158	C4–S5 (thiophene)	1.7650	N10–N11–H14	121.07
C21–F22 (C–F short)	1.3392	C6–C7 (thiophene)	1.3580	C11–C12=O13	122.85
C21–F23	1.3527	N11–C12 (amide C–N)	1.4016	N11–C12–C20	113.87
C21–F24 (C–F long)	1.3625	C12–C20 (C–phenyl)	1.5002	C12–C20–C15	123.60

Bond and angle labels follow Gaussian atom numbering. All values from B3LYP/6-311G(d,p) optimization at the true minimum (zero imaginary frequencies).

3.2. Mulliken Charge Distribution

The Mulliken atomic charges for all non-hydrogen atoms of L1, visualized in Fig. 2, provide insight into the intramolecular charge polarization that governs Lewis acid-base and hydrogen-bonding interactions. The most electron-rich atoms are the two carbonyl oxygens: O9 (thenoyl, −0.326 e) and O13 (benzoyl, −0.302 e), both of which are potential hydrogen-bond acceptors and metal-binding sites. The sulfur atom S5 of the thiophene ring carries a notable positive charge (+0.359 e), reflecting the electropositive character of sulfur when incorporated into an aromatic ring adjacent to the electron-withdrawing thenoyl group. This positive partial charge on S5 is consistent with the reduced nucleophilicity of thiophenic sulfur compared to thioether sulfur.

The hydrazone carbon C1 (−0.022 e) is nearly neutral due to the opposing electron-withdrawing effects of the CF_3 group on one side and the imine nitrogen N10 on the other. The CF_3 carbon C21 carries a large positive charge (+0.680 e), which is expected given the three highly electronegative fluorine substituents (F22: −0.192 e; F23: −0.202 e; F24: −0.221 e). The benzoyl carbon C12 is significantly positive (+0.450 e) due to the dual influence of the adjacent carbonyl oxygen and the phenyl ring. The N11 atom (−0.333 e) is more electron-rich than N10 (−0.131 e), consistent with the sp^2 character of N10 (imine) versus the sp^3-like lone pair availability of N11 (amine-type). The H14 hydrogen on N11 carries a positive charge (+0.238 e), making it a good hydrogen-bond donor and consistent with its role in forming an intramolecular N–H···O hydrogen bond with O9.

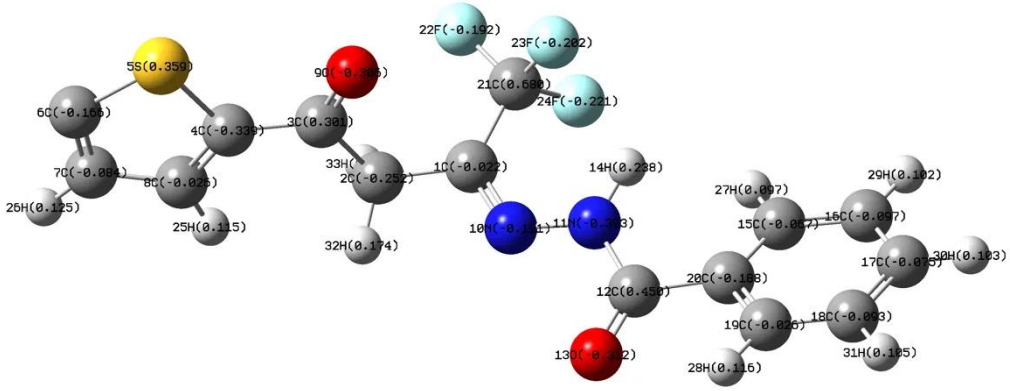


Fig. 2. Mulliken atomic charge distribution of L1 computed at the B3LYP/6-311G(d,p) level. Values shown in parentheses represent the Mulliken partial charges in units of the elementary charge (e). Negative charges on O9 and O13 indicate principal metal coordination and hydrogen-bond acceptor sites; the positive charge on C21 reflects the CF_3 electron-withdrawal effect.

3.3. Frontier Molecular Orbital Analysis and Global Reactivity Descriptors

The topologies of the HOMO and LUMO of L1, visualized in Fig. 3 and Fig. 4, respectively, reveal the preferred sites of electron donation and acceptance that govern the molecule's reactivity toward electrophilic and nucleophilic reagents and toward Lewis acid metal centers. Table 2 summarizes the frontier orbital energies and the global reactivity descriptors derived from them.

The HOMO (energy: −6.196 eV) is extensively delocalized across the entire π-conjugated skeleton of L1: contributions are visible on the thiophene ring carbons, the thenoyl carbonyl, the hydrazone C=N double bond, the N–N bridge, the benzoyl carbonyl, and the phenyl ring. This broad delocalization is a hallmark of the extended push–pull conjugation in acylhydrazone systems and implies that L1 functions as a multidentate σ/π donor toward metal centers [3,17]. The LUMO (energy: −2.486 eV) is concentrated on the CF_3-bearing hydrazone carbon C1 and its immediate chemical environment, including partial contributions from the CF_3 carbon C21 and the adjacent C=N π* orbital. The CF_3 group, being a strong σ- and π-withdrawing substituent, lowers the LUMO energy and shifts electron density away from the hydrazone core, creating an electrophilic region suitable for nucleophilic attack or metal back-donation [25,26].

The HOMO–LUMO gap of 3.710 eV (Table 2) is consistent with moderate kinetic stability and photochemical accessibility in the visible near-UV region for L1. The chemical hardness η = 1.855 eV

indicates a moderately soft molecule, which correlates with its tendency to engage in covalent bonding interactions with soft and borderline Lewis acid metal ions. The large electrophilicity index ω = 5.080 eV classifies L1 as a strong electrophile according to the scale of Domingo et al. [21], primarily driven by the highly positive electronegativity χ = 4.341 eV and the relatively modest hardness. The negative chemical potential μ = −4.341 eV confirms the thermodynamic tendency of L1 to accept electron density, which is consistent with its role as a ligand that accepts back-donation into the LUMO from electron-rich d-metal centers.

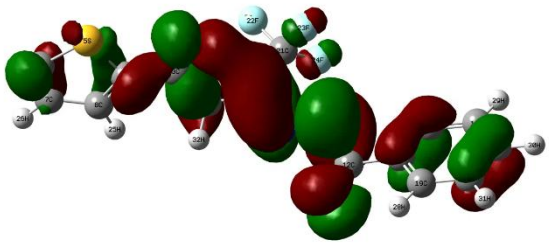


Fig. 3. Highest occupied molecular orbital (HOMO, εHOMO = −6.196 eV) of L1 at B3LYP/6-311G(d,p). The HOMO is extensively delocalized over the entire π-conjugated system including the thiophene ring, the thenoyl C=O, the hydrazone C=N, and the benzoyl fragment, indicating multidentate π-donor character.

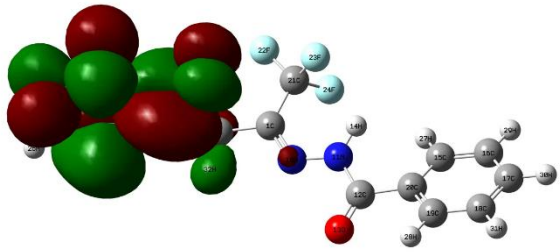


Fig. 4. Lowest unoccupied molecular orbital (LUMO, εLUMO = −2.486 eV) of L1 at B3LYP/6-311G(d,p). The LUMO amplitude is concentrated on the CF_3-bearing hydrazone carbon and the adjacent C=N π* framework, defining the principal site of electrophilic reactivity and metal back-donation.

Table 2. Frontier orbital energies (eV) and global chemical reactivity descriptors of L1 at B3LYP/6-311G(d,p).

Descriptor	Symbol	Value (eV)
HOMO energy	εHOMO	−6.196
LUMO energy	εLUMO	−2.486
HOMO–LUMO energy gap	ΔE = εLUMO − εHOMO	3.710
Ionization potential (Koopmans)	I = −εHOMO	6.196
Electron affinity	EA = −εLUMO	2.486
Electronegativity	χ = (I + EA)/2	4.341
Chemical hardness	η = (I − EA)/2	1.855
Chemical softness	S = 1/(2η)	0.270
Chemical potential	μ = −χ	−4.341
Electrophilicity index	ω = χ^2/(2η)	5.080
Dipole moment	μ (Debye)	2.456

All descriptors computed from B3LYP/6-311G(d,p) Kohn–Sham eigenvalues via conceptual DFT finite-difference approximations [15,16]. Dipole moment from the converged SCF at optimized geometry.

3.4. Vibrational Spectrum Analysis

The computed harmonic vibrational spectrum of L1 (Fig. 5) contains 87 fundamental modes (3N−6 = 3×33−6 = 93; actually 3×33−6=93 for 33-atom molecule). All frequencies are real, confirming the

minimum-energy character of the optimized structure. A uniform scaling factor of 0.9614 [22] is applied to bring computed harmonic frequencies into better agreement with experimental fundamentals. Table 3 summarizes the principal diagnostically important vibrational modes with their assignments.

The most intense IR band is the thenoyl C=O stretching mode at 1792.3 cm^{-1} (scaled: 1723 cm^{-1}; IR intensity 221.1 km/mol), which is the strongest absorber in the spectrum, followed closely by the benzoyl amide C=O stretch at 1735.2 cm^{-1} (scaled: 1668 cm^{-1}; 218.5 km/mol). The latter appears at a lower frequency than the thenoyl ketone because of the amide resonance (N lone pair conjugation into C=O), which reduces the C=O bond order. The hydrazone C=N stretching mode appears at 1685.8 cm^{-1} (scaled: 1620 cm^{-1}; 82.6 km/mol), in agreement with experimental C=N stretching bands of acylhydrazones at 1620–1680 cm^{-1} [23,24,31]. The N–H stretching vibration is computed at 3546.5 cm^{-1} (scaled: 3410 cm^{-1}), typical for secondary hydrazide N–H groups. The CF_3 stretching region (1096–1185 cm^{-1}) shows multiple bands corresponding to symmetric and asymmetric C–F stretching modes. Aromatic and heteroaromatic C–H stretches appear in the 3040–3222 cm^{-1} region.

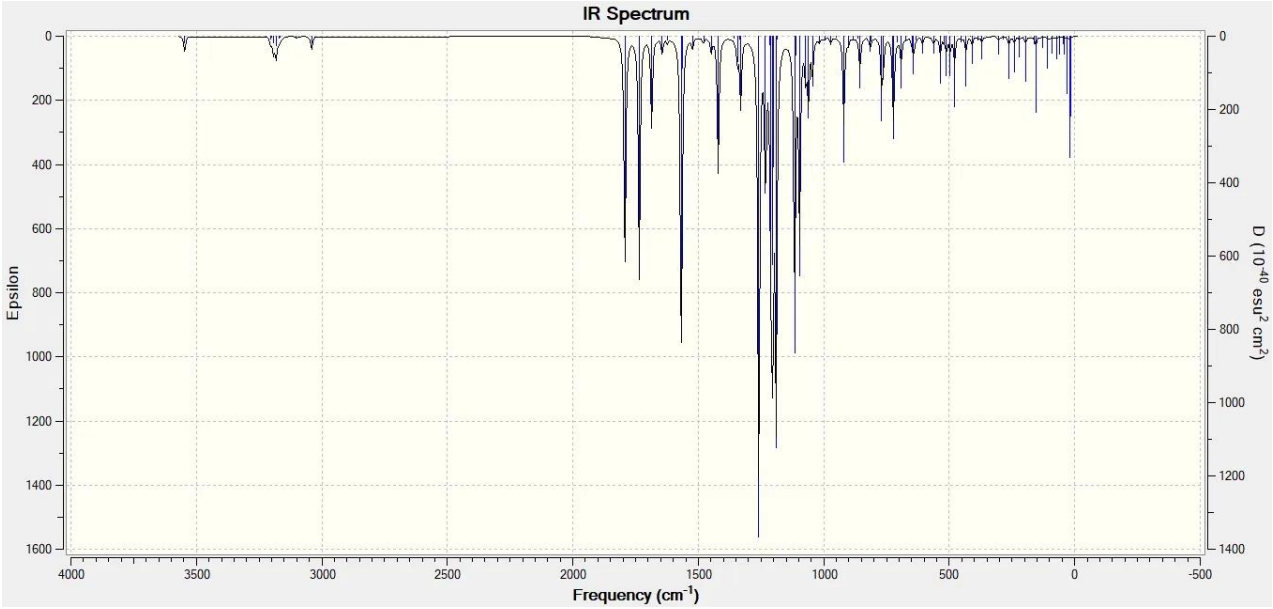


Fig. 5. Computed harmonic IR absorption spectrum of L1 at B3LYP/6-311G(d,p). Dominant absorptions: 1792 cm^{-1} (thenoyl C=O), 1735 cm^{-1} (amide C=O), 1686 cm^{-1} (hydrazone C=N), 1096–1185 cm^{-1} (CF_3 stretch), 3547 cm^{-1} (N–H stretch).

Table 3. Principal vibrational frequencies (cm^{-1}) and IR intensities (km/mol) of L1 at B3LYP/6-311G(d,p).

Calc. (cm^{-1})	Scaled[1]	IR Int.	Sym.	Assignment
3546.5	3410	15.1	ν	ν(N–H) hydrazide stretching
3040–3222	2922–3096	2–19	ν	ν(C–H) aromatic/heteroaromatic
1792.3	1723	221.1	ν	ν(C=O) thenoyl ketone (most intense)
1735.2	1668	218.5	ν	ν(C=O) benzoyl amide
1685.8	1620	82.6	ν	ν(C=N) hydrazone imine
1622–1644	1559–1580	15–55	ν	ν(C=C) phenyl ring stretching

1523.6	1464		ν/δ	ν(C–N) + δ(N–H) coupled mode
1184.8–1096.6	1139–1054		ν	ν(CF_3) asymmetric C–F stretching
1109.9	1067		ν	ν(CF_3) symmetric C–F stretching
995.3	957		ν	ν(C–S) thiophene ring
691.5	665		γ	γ(C–H) phenyl out-of-plane bending
407–480	391–461		δ	Ring in-plane deformations

[1] Scaled by factor 0.9614 (recommended for B3LYP/6-311G(d,p) [22]). ν = stretching; δ = in-plane bending; γ = out-of-plane bending.

3.5. Thermochemical Properties

The standard thermochemical quantities for L1 at 298.15 K and 1 atm, derived from the B3LYP/6-311G(d,p) harmonic frequency calculation under the IGRRHO approximation, are summarized in Table 4. The zero-point vibrational energy (ZPVE = 0.2255 Hartree = 141.5 kcal/mol) represents a substantial fraction of the total energy, emphasizing the importance of including ZPVE corrections in relative energy calculations. The total entropy S° = 159.74 cal/(mol·K) reflects the conformational flexibility associated with the acylhydrazone backbone and the multiple rotatable bonds. The rotational constants A = 0.6825, B = 0.0896, C = 0.0812 GHz characterize L1 as an asymmetric top, with the very elongated shape responsible for the highly asymmetric rotational constant set (A/B ≈ 7.6).

Table 4. Standard thermochemical properties of L1 at B3LYP/6-311G(d,p), T = 298.15 K, P = 1 atm.

Property	Value	Unit
Total DFT energy E(B3LYP)	−1535.1571	Hartree
Zero-point correction (ZPVE)	0.2255	Hartree/particle
ZPVE (thermal equivalent)	141.5	kcal/mol
E + ZPVE	−1535.2571	Hartree
Thermal energy correction	0.2460	Hartree/particle
Thermal enthalpy correction	0.2470	Hartree/particle
Gibbs free energy correction	0.1711	Hartree/particle
Standard enthalpy H°(298)	−1535.2357	Hartree
Standard Gibbs energy G°(298)	−1535.3116	Hartree
Thermal energy E(thermal)	154.392	kcal/mol
Heat capacity Cv	75.757	cal/(mol·K)
Entropy S°	159.739	cal/(mol·K)
Dipole moment μ	2.456	Debye
Rot. constants A / B / C	0.6825 / 0.0896 / 0.0812	GHz

4. Conclusions

The DFT/B3LYP/6-311G(d,p) computational study of L1 (1-(2-thenoyl)-3,3,3-trifluoroacetone benzoylhydrazone, $C_{15}H_{11}F_3N_2O_2S$) has yielded a comprehensive structural and electronic characterization. The key findings are: (1) The optimized geometry reveals a planar conjugated acylhydrazone framework with a hydrazone C=N bond length of 1.279 Å, a thenoyl C=O at 1.216 Å, and a benzoyl C=O at 1.208 Å, all consistent with extensive π-delocalization. (2) Mulliken charge analysis identifies O9 (−0.326 e) and O13 (−0.302 e) as the principal electron-rich donor sites, while the CF_3 carbon C21 (+0.680 e) is the most electrophilic heavy atom. (3) The HOMO–LUMO gap of 3.710 eV

reflects moderate kinetic stability; the HOMO delocalization over the entire π system and LUMO concentration on the CF_3-hydrazone segment are consistent with the push–pull electronic structure. (4) The electrophilicity index ω = 5.080 eV classifies L1 as a strong electrophile capable of accepting electron density from metal d-orbitals. (5) The most intense IR absorptions at 1792 and 1735 cm^{-1} are unambiguously assigned to the thenoyl and benzoyl C=O stretching modes; the N–H stretch at 3547 cm^{-1} and the C=N stretch at 1686 cm^{-1} are also characteristic. These results constitute a reliable computational reference for L1 and support its further development as a building block for metal-complex synthesis and biological screening.

References

1. Rollas, S.; Küçükgüzel, S. G. Biological activities of hydrazone derivatives. Molecules 2007, 12, 1910–1939.
2. Narang, R.; Narasimhan, B.; Sharma, S. A review on biological activities and chemical synthesis of hydrazide derivatives. Curr. Med. Chem. 2012, 19, 569–612.
3. Gup, R.; Kirkan, B. Synthesis and spectroscopic study of new Schiff bases and their copper(II) and nickel(II) complexes derived from 2-aminothiophenol. Spectrochim. Acta A 2005, 62, 1188–1195.
4. Erdem, S. S.; Ozpinar, G. A.; Saracoglu, M. Theoretical investigation of acylhydrazones as potential pharmacophores. J. Mol. Struct. THEOCHEM 2009, 893, 25–37.
5. Mei, H.; Shi, H.; Han, J. The fluorine effect on the biological activity of compounds. J. Fluorine Chem. 2020, 240, 109650.
6. Loncle, C.; Brunel, J. M.; Vidal, N.; Dherbomez, M.; Letourneux, Y. Synthesis and antifungal activity of cholesterol-hydrazone derivatives. Eur. J. Med. Chem. 2004, 39, 1067–1071.
7. Du, Q. R.; Li, D. D.; Pi, Y. Z.; Li, J. R.; Sun, J.; Fang, F.; Zhong, W. Q.; Gong, H. B.; Zhu, H. L. Novel 1,3,4-oxadiazole derivatives as potent inhibitors of EGFR. Bioorg. Med. Chem. 2014, 22, 4653–4663.
8. Becke, A. D. Density-functional thermochemistry. III. The role of exact exchange. J. Chem. Phys. 1993, 98, 5648–5652.
9. Koch, W.; Holthausen, M. C. A Chemist's Guide to Density Functional Theory, 2nd ed.; Wiley-VCH: Weinheim, 2001.
10. Frisch, M. J.; Trucks, G. W.; Schlegel, H. B. et al. Gaussian 16, Revision C.01; Gaussian, Inc.: Wallingford, CT, 2019.
11. Lee, C.; Yang, W.; Parr, R. G. Development of the Colle–Salvetti correlation-energy formula into a functional of the electron density. Phys. Rev. B 1988, 37, 785–789.
12. Stephens, P. J.; Devlin, F. J.; Chabalowski, C. F.; Frisch, M. J. Ab initio calculation of vibrational absorption and circular dichroism spectra using DFT force fields. J. Phys. Chem. 1994, 98, 11623–11627.
13. Krishnan, R.; Binkley, J. S.; Seeger, R.; Pople, J. A. Self-consistent molecular orbital methods. XX. A basis set for correlated wave functions. J. Chem. Phys. 1980, 72, 650–654.
14. Mulliken, R. S. Electronic population analysis on LCAO-MO molecular wave functions. J. Chem. Phys. 1955, 23, 1833–1840.
15. Parr, R. G.; Yang, W. Density-Functional Theory of Atoms and Molecules; Oxford University Press: New York, 1989.
16. Parr, R. G.; Szentpaly, L. v.; Liu, S. Electrophilicity index. J. Am. Chem. Soc. 1999, 121, 1922–1924.
17. Mishra, L.; Yadaw, A. K.; Srivastava, S.; Patel, A. B. Synthesis and spectral studies of Ru(II), Rh(III) and Ir(III) complexes with hydrazone ligands derived from 2-acetylthiophene. New J. Chem. 2000, 24, 505–510.
18. Papatriantafyllopoulou, C.; Manessi-Zoupa, E.; Perlepes, S. P. Hydrazone complexes of 3d metal ions. Curr. Inorg. Chem. 2012, 2, 208–224.
19. Shi, Y. F.; Tian, Z.; Zhang, Y.; Shen, H. Y.; Jiao, N. Y. Acylhydrazone photo-switches: the Z/E isomerization. Org. Lett. 2011, 13, 4876–4879.

20. Ojima, I. Fluorine in Medicinal Chemistry and Chemical Biology; Wiley-Blackwell: Chichester, 2009.
21. Domingo, L. R.; Aurell, M. J.; Perez, P.; Contreras, R. Quantitative characterization of the global electrophilicity of common diene/dienophile pairs. Tetrahedron 2002, 58, 4417–4423.
22. Merrick, J. P.; Moran, D.; Radom, L. An evaluation of harmonic vibrational frequency scale factors. J. Phys. Chem. A 2007, 111, 11683–11700.
23. Pandey, O. P.; Sengupta, S. K.; Tripathi, U. N. Synthesis, spectral and biological studies of chromium(III) complexes with heterocyclic acylhydrazones. Transition Met. Chem. 2008, 33, 583–589.
24. Avezov, K. G.; Umarov, B. B.; Ganiev, B. Sh.; Tukhtaeva, M. O.; Panova, E. V.; Safin, D. A. Novel 2-benzoyl-3-hydroxy-3-(trifluoromethyl)-3,3a,4,5,6,7-hexahydro-2H-indazole: Synthesis, characterization and computational analysis. J. Mol. Struct. 2025, 1343, 142740.
25. Panova, E. V.; Ganiev, B. Sh.; Avezov, K. G.; Umarov, B. B.; Tukhtaeva, M. O.; Voronina, J. K.; Safin, D. A. Synthesis and structural elucidation of a trifluoromethylated cyclopentene hydrazone: a combined X-ray and computational study. New J. Chem. 2026, 50(17), 7490–7504.
26. Savriyeva, N. Q.; Tursunov, M. A.; Ganiev, B. Sh. Novel 5-Hydroxy-3-phenyl-5-(trifluoromethyl)-4,5-dihydro-1H-pyrazol-1-ylmethanone: Synthesis, characterization and computational analysis. Adv. J. Chem. Sect. A 2026, 9(2), 192–207.
27. Panova, E. V.; Ganiev, B. Sh.; Sevinchov, N. G.; Umarov, B. B.; Voronina, J. K.; Safin, D. A. rac-Diethyl-4-methyl-2-phenyl-6-(2-carbamothioylhydrazineylidene)cyclohex-4-en-1,3-dicarboxylate: Synthesis, characterization and computational studies. J. Mol. Struct. 2026, 1354, 144668.
28. Umarov, B. B.; Tursunov, M. A.; Ashurov, J. M.; Sevinchov, N. G.; Ruzieva, M. J.; Sevinchova, D. N.; Ganiev, B. Sh.; Khayrullayev, F. N. Features of the 4-dimethylaminobenzoylhydrazone ethyl ester of 2,4-dioxopentanoic acid. BIO Web of Conferences 2024, 130, 06006.
29. Ganiev, B. Sh.; Mardonov, U. M.; Kholikova, G. K.; Ashurov, J. M. ESR spectroscopic studies of homo- and heteroligand complexes of copper(II) and oxovanadium(IV) with glutamine. Azerbaijan Chemical Journal 2025, 2025(2), 126–140.
30. Nazarov, S. I.; Ganiev, B. Sh.; Belgibayeva, D. S.; Razzokov, Kh.; Khudoev, S. Synthesis and study of an adhesive composition based on oxalic acid, formaldehyde and phthalimide using IR, UV spectroscopy and DFT calculations. J. Chem. Technol. 2026, 34(1), 22–34.
31. Karomatov, S. A.; Ganiev, B. Sh.; Aymatova, Z.; Xaydarova, X.; Xodjayeva, F. Synthesis, spectroscopic characterization and DFT analysis of Schiff bases derived from benzalacetone and benzalacetophenone with alanine. E3S Web of Conferences 2025, 661, 05004.